Dispersion of Self-Propelled Rods Undergoing Fluctuation-Driven Flips

Daisuke Takagi,[1] Adam B. Braunschweig,[2] Jun Zhang,[1,3] and Michael J. Shelley[1]
[1]*Applied Math Lab, Courant Institute, New York University, New York, New York 10012, USA*
[2]*Department of Chemistry, New York University, New York, New York 10003, USA*
[3]*Department of Physics, New York University, New York, New York 10003, USA*
(Received 14 August 2012; published 15 January 2013)

Synthetic microswimmers may someday perform medical and technological tasks, but predicting their motion and dispersion is challenging. Here we show that chemically propelled rods tend to move on a surface along large circles but curiously show stochastic changes in the sign of the orbit curvature. By accounting for fluctuation-driven flipping of slightly curved rods, we obtain analytical predictions for the ensemble behavior in good agreement with our experiments. This shows that minor defects in swimmer shape can yield major long-term effects on macroscopic dispersion.

DOI: 10.1103/PhysRevLett.110.038301 PACS numbers: 82.70.−y, 05.40.−a, 47.57.eb, 47.63.Gd

Micro- and nanoscale motors are envisioned to be used in numerous applications [1–4], including biosensing and drug delivery in medicine [5], flow control and mixing in microfluidics [6], and cargo transport and assembly in nanotechnology [7]. A prototype motor consists of a bimetallic rod that can be propelled in a fluid of chemical fuel [8]. Recent studies have focused on the synthesis of rods with different material compositions to propel them in various fuels [9–13]. Trajectories with linear, circular, and undulatory patterns have been observed near surfaces [10,14,15], and the particle shape has been recognized as a factor [16–18], but a general understanding of how microscopic features of swimmers affect macroscopic behavior is not yet complete.

Here we show that, while even a slight curvature in chemically propelled rods gives them curved orbits when moving on a surface, it also gives them two stable states between which they can stochastically switch due to thermal fluctuations. This greatly affects their dynamics, specifically their directional changes, displacement, and diffusion over time. We develop, without fitting parameters, a two-state Fokker-Planck description from which we make analytical predictions of ensemble quantities such as the persistence time and particle diffusivity. These quantities are measured in our experiments and validate our theory, which is also used to make predictions of aggregation in low-fuel regions.

We fabricated rods of length $L = 2.0 \pm 0.2$ μm and diameter $2R = 0.39 \pm 0.04$ μm [Figs. 1(a) and 1(b)], consisting of platinum (Pt) and gold (Au) segments, by electrochemical deposition in anodic aluminum oxide templates using a previously reported method [19,20]. These rods move autonomously in hydrogen peroxide (H_2O_2) solutions through a local flux of ions which arises from two paired redox reactions on the metal surfaces [21]. The positions of ~100 rods, moving independently along the surface of a microscope slide, were tracked at 9 frames per second for up to 150 seconds (10× objective lens of a Nikon Eclipse 80i microscope and Lumenera Infinity 1-3 camera) to analyze trajectories. Varying the ratio of Pt to Au between 1/3 and 3 did not affect any of the results reported here, but increase of the H_2O_2 concentration C (up to 25%) gave an approximately linear increase in swimming speed.

By altering C and thereby the speed, the trajectory patterns become strikingly different. Unlike slow rods, which change direction stochastically through thermal fluctuations [Fig. 1(c)], fast rods tend to change direction coherently in circular orbits [Fig. 1(d)]. Both clockwise (CW) and counterclockwise (CCW) orbits are observed with various radii depending on each rod, as shown by summing the path curvature along trajectories [Fig. 2(a)].

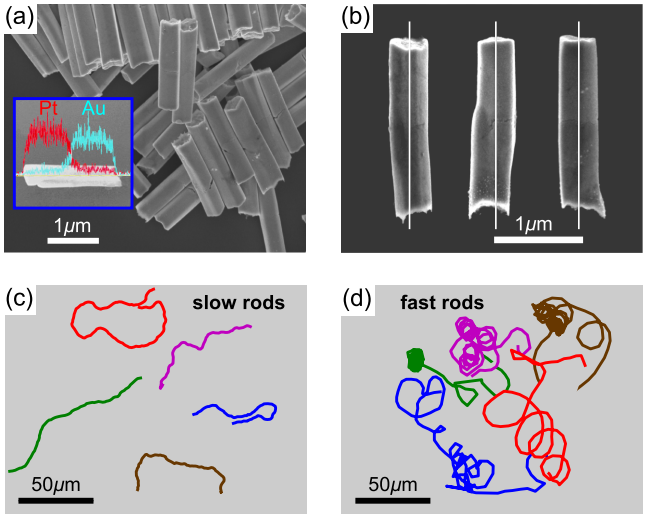

FIG. 1 (color online). Structure and trajectory patterns of Au-Pt rods. (a) Scanning electron microscopy image of rods (Zeiss Merlin scanning electron microscope). The inset shows the presence of Au and Pt segments confirmed by energy-dispersive x-ray spectroscopy. (b) The rods are not perfectly axisymmetric in shape. Representative trajectories of (c) slow rods (average speed $U \sim 8$ μm s^{-1}) and (d) fast rods ($U \sim 39$ μm s^{-1}) tracked over 15 seconds.

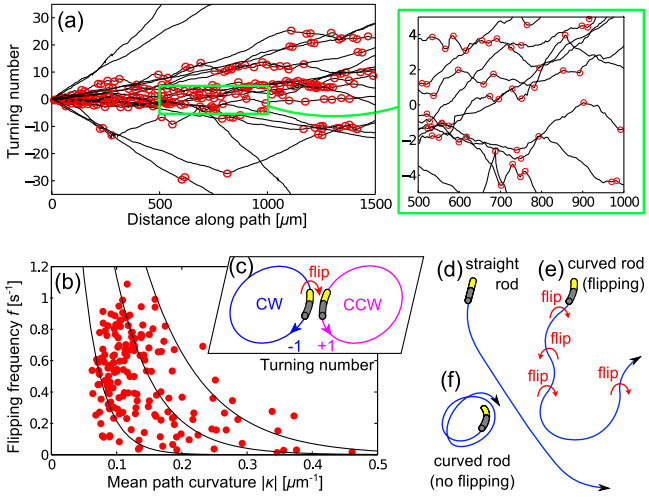

FIG. 2 (color online). Turning and flipping rods. (a) Turning number, defined as the cumulative sum of the path curvature divided by 2π, plotted for 20 fast rods (average speed $\sim 38\ \mu\mathrm{m\,s^{-1}}$). Open circles represent flips, defined to have occurred when the sign of the path curvature switches and then stays the same for at least three frames. (b) Frequency of flips plotted against $|\kappa|$, estimated for each rod by averaging the absolute change in total curvature divided by the distance traveled between flips. The solid lines are given by Eq. (1) with $h_0 = 5$, 10, 15 nm from left to right, respectively. (c) Sketch of curved rods flipping between CW and CCW orbits. (d) A straight rod moves along a series of straight paths. (e) A slightly curved rod turns and flips. (f) A highly curved rod turns without flipping.

Sign changes in the path curvature indicate that rods switch spontaneously between moving in CW and CCW orbits. The switches occur less frequently for rods moving in tighter orbits [Fig. 2(b)].

To explore whether the orbits are caused by minor imperfections in the rods, which include slight curvatures, irregular interfaces between Au and Pt, and asperities at the ends, we propose a simple theory assuming that the rods are slightly curved. We consider a rod with constant curvature $\hat{\kappa}$ and a prescribed slip velocity along its elongated body in the bulk fluid. By using the slender body theory for a particle in Stokes flow [22] and imposing force-free and torque-free conditions, a linear system can be obtained for the position and orientation of the rod. Their solution shows that the rod follows a curved path with curvature κ comparable to $\hat{\kappa}$. The slightly curved rods [Fig. 1(b)] and their orbits [Fig. 2(a)] are consistent with $\hat{\kappa} = 0.12 \pm 0.04\ \mu\mathrm{m^{-1}}$ in this simplified theory.

Why do rods switch spontaneously between moving in CW and CCW orbits? This curious phenomenon can be explained by assuming that the metallic rods are moving close to a horizontal surface. Unlike in the bulk fluid, where the rods are free to rotate continuously about their direction of motion, the presence of the surface restricts the rods to lie on one side or the other [Fig. 2(c)] so as to minimize the gravitational potential energy. Curved rods can flip and switch sides only by rotating and lifting their center of mass by a height $\Delta h \sim \hat{\kappa} L^2/24$, which is about 20 nm for rods with typical curvature $\hat{\kappa} \sim 0.12\ \mu\mathrm{m^{-1}}$. For synthetic microswimmers, thermal fluctuations are sufficient to cause spontaneous flips by raising the height from a base level h_0. The flipping frequency has the form

$$f = f_0 e^{-\Delta h/h_0}, \tag{1}$$

where $f_0 \sim 6\ \mathrm{s^{-1}}$ is the rotation rate around the axis of a straight rod, estimated from the time scale of rotational diffusion of a prolate spheroid of comparable size [23]. Equation (1) with $h_0 \sim 10$ nm shows that a slight curvature in the rods significantly suppresses the flipping frequency in agreement with our experimental data [Fig. 2(b)]. The strong dependence of flipping on apparent rod curvature is consistent with self-propelled rods moving at a height $h_0 \sim 10$ nm above the substrate. This height has the same order of magnitude as the expected sedimentation height of passive rods in thermal equilibrium $k_B T/2mg \sim 40$ nm, where k_B is the Boltzmann constant, T is the room temperature, m is the mass of the rod, and g is the gravitational acceleration. However, such small distances cannot be resolved by using optical microscopy. Perhaps, chemical reactions and self-propulsion could change the *effective* temperature of this out-of-equilibrium system and so change the sedimentation height of self-propelled rods. It would seem likely, though, that our curved rods are no more than 20 nm above the surface for them to show a flipping dynamics between two states as in our observations [24].

What are the long-term implications of flipping? Minor variations in rod curvature lead to major changes in trajectory patterns [Figs. 2(d)–2(f)] and affect dispersion. To gain quantitative insight into the long-term effects of flipping, we formulate a two-dimensional model of flipping rods with translational and rotational diffusion coefficients $\bar{D}$ and D_r, respectively. The difference in translational diffusions along and across the rod axis is neglected for simplicity. In the absence of thermal fluctuations, each rod is assumed to translate with speed U in the axial direction $\mathbf{n} = (\cos\theta, \sin\theta)$ and turn with angular speed $U\kappa$. The rods tend to follow paths with curvature κ taking either of the two values $\pm\kappa_0$, where the sign switches at a characteristic rate f. The center of mass $\mathbf{x} = (x, y)$, the orientation angle θ, and the curvature κ are evolved over time step Δt according to the stochastic equations of motion

$$\mathbf{x}(t + \Delta t) - \mathbf{x}(t) = U\mathbf{n}[\theta(t)]\Delta t + \sqrt{2\bar{D}\Delta t}\mathbf{X}, \tag{2}$$

$$\theta(t + \Delta t) - \theta(t) = U\kappa(t)\Delta t + \sqrt{2D_r\Delta t}\Theta, \tag{3}$$

$$\kappa(t + \Delta t) - \kappa(t) = -2\kappa(t)B, \tag{4}$$

where the components of $\mathbf{X}$ and Θ are random variables with a standard normal distribution and B is a Bernoulli random variable with success probability $f\Delta t$. Up to 500 particles are simulated with various prescribed speeds U and fixed parameter values $\bar{D} = 0.3\ \mu\mathrm{m}^2\,\mathrm{s}^{-1}$, $D_r = 1.0\ \mathrm{s}^{-1}$, and $\kappa_0 = 0.12\ \mu\mathrm{m}^{-1}$, which are all estimated from our experiments, and $f = 0.9\ \mathrm{s}^{-1}$ estimated by using Eq. (1). The results are incorporated into Figs. 3(b) and 4(b) described below. To study the ensemble behavior, we represent the configuration of rods by the probability distribution functions [25] $\Psi_\pm(\mathbf{x}, \theta, \pm\kappa_0, t)$, which evolve according to the Fokker-Planck equation associated with the Langevin equations (2)–(4). The evolution is described by the conservation equation

$$\frac{\partial \Psi_\pm}{\partial t} + \nabla\cdot(\dot{\mathbf{x}}\Psi_\pm) + \frac{\partial}{\partial\theta}(\dot{\theta}\Psi_\pm) = f(\Psi_\mp - \Psi_\pm), \quad (5)$$

where $\dot{\mathbf{x}} = U\mathbf{n}(\theta) - \bar{D}\nabla\log\Psi_\pm$, $\dot{\theta} = \pm U\kappa_0 - D_r\frac{\partial}{\partial\theta}\log\Psi_\pm$. Important ensemble quantities, such as the expected change in orientation and mean-square displacement (MSD) over time, can be derived analytically from Eq. (5) and compared directly with our experiments.

This model is different from earlier models of synthetic microswimmers, which are commonly assumed to undergo a succession of straight directed runs followed by random changes in direction [15,26]. Our model is similar to that for "circle swimmers" [27] experiencing an effective Lorentz force, except that in ours the angular velocity switches between two discrete values. This same switching process was formulated independently [28] in a model of the zooplankton *Daphnia* [29], and a particular generalization of this model was developed recently to calculate effective diffusivity [30].

To test our model against experiments, first consider the time-dependent expected change in orientation of three sets of rods moving at different speeds [Fig. 3(a)]. The experimental data decay over time in good agreement with our prediction

$$\langle\cos\Delta\theta\rangle(t) = \mathrm{Re}\{c_+ e^{-\sigma_+ f t} + c_- e^{-\sigma_- f t}\}, \quad (6)$$

where $\langle\cdot\rangle = \int_\Omega dA_{\mathbf{x}} \int_0^{2\pi} d\theta(\Psi_+ + \Psi_-)$, $\sigma_\pm = 1 + D_r/f \pm \sqrt{\lambda}$, $c_\pm = (1 \mp \lambda^{-1/2})/2$, and $\lambda = 1 - (U\kappa_0/f)^2$. Equation (6) is obtained by solving a linear system of ordinary differential equations for $\langle\cos\Delta\theta\rangle(t)$ and $\langle\kappa\sin\Delta\theta\rangle(t)$, which follow from multiplying Eq. (5) by $\cos\Delta\theta$ and separately by $\kappa\sin\Delta\theta$ and then integrating over θ and $\mathbf{x}$. For fast rods with $\lambda < 0$, the real part of Eq. (6) is taken and exhibits oscillatory behavior. The time when $\langle\cos\Delta\theta\rangle$ decays to e^{-1} gives a measure of the typical time needed for rods to change orientations (persistence time), which is shown in Fig. 3(b) for rods moving at various speeds in our experiments, simulations, and theory. The persistence time decreases systematically with smaller error bars at higher speeds, which can be explained only by assuming that the rods are curved. Contrary to slow rods, which change direction stochastically through thermal fluctuations, sufficiently fast rods change direction deterministically and more rapidly because of their intrinsic curvature.

The model is tested further by measuring the time-dependent MSD of rods with different speeds, controlled by varying C in six different experiments [Fig. 4(a)]. Self-propelled rods exhibit nearly ballistic behavior over short times and diffusive behavior over times longer than about a second, all in excellent agreement with our prediction

$$\langle\Delta\mathbf{x}^2\rangle(t) = 4Dt + \mathrm{Re}\{d_+(e^{-\sigma_+ f t} - 1) + d_-(e^{-\sigma_- f t} - 1)\}, \quad (7)$$

where $d_\pm = (1 - \lambda)(1 \mp \lambda^{-1/2})/(\sigma_\pm^2\kappa_0^2)$ and

$$D = \bar{D} + \frac{U^2(D_r + 2f)}{2U^2\kappa_0^2 + 2D_r(D_r + 2f)} \quad (8)$$

is the effective diffusion coefficient or diffusivity. Equation (7) is obtained by solving a linear system of ordinary differential equations for $\langle\mathbf{x}^2\rangle(t)$, $\langle\mathbf{x}\cdot\mathbf{n}\rangle(t)$, and

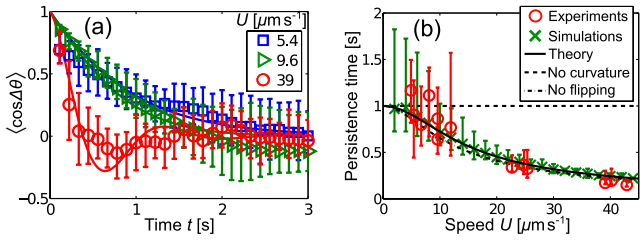

FIG. 3 (color online). Measured and predicted changes in the direction of self-propelled rods. (a) Correlation in the direction of three sets of rods moving at different speeds U. Experimental data (symbols) have error bars representing lower and upper quartiles. Corresponding predictions (lines) are given by Eq. (6). (b) The persistence time and its error bars decrease with speed in our experiments (circles), simulations (crosses), and theory (solid line).

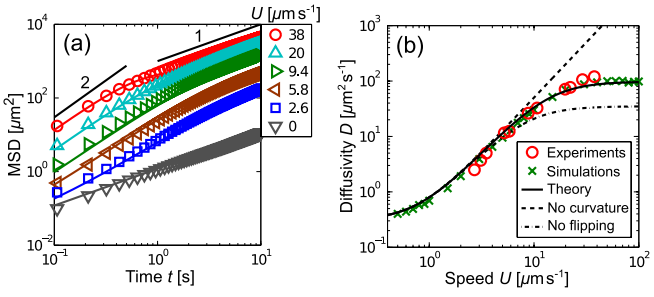

FIG. 4 (color online). Measured and predicted diffusion of rods. (a) MSD of rods moving at various speeds in six different experiments (symbols). Predictions (lines) are given by Eq. (7). (b) The diffusivity saturates with increasing speed in our experiments (circles), simulations (crosses), and theory (solid line). Theoretical curves are given by Eq. (8) with $\kappa_0 = 0$ for no curvature and $f = 0$ for no flipping.

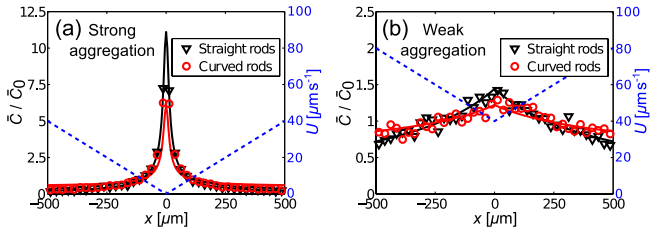

FIG. 5 (color online). Long-time swimmer concentrations $\bar{C}$ (symbols and solid lines) in chemical fuel gradients. Swimming speeds $U(x)$ (blue dashed lines) are prescribed and range from (a) 0 to 40 or (b) 40 to 80 $\mu\mathrm{m\,s^{-1}}$. Symbols show simulations of straight and curved rods 30 minutes after initiating with uniform distribution $\bar{C}_0$. Solid lines are corresponding numerical solutions to the steady form of Eq. (5).

$\langle \kappa \mathbf{x} \cdot d\mathbf{n}/d\theta \rangle(t)$, which are all derived from Eq. (5) like in the earlier derivation of Eq. (6). The diffusivity of rods moving at various speeds is shown in Fig. 4(b), estimated by averaging $\langle \Delta \mathbf{x}^2 \rangle / 4t$ for large times in our experiments and simulations. The diffusivity is overestimated if the rods are assumed to move in a series of straight paths [15,26] and underestimated if the rods are assumed to turn without flipping [27]. However, the data agree quantitatively with Eq. (8) after incorporating the effects of flipping. The diffusivity saturates with increasing speed, because faster rods remain localized by completing more orbits, but our model shows that the diffusivity can be enhanced with more frequent flips.

Having been validated against experiments, our model can be used to make predictions of how ensembles of microswimmers migrate in spatially varying environments. As an example, the long-term effects of a spatial gradient in fuel concentration are demonstrated. Since the swimming speed varies linearly with H_2O_2 concentration, U is prescribed as a function of space in our model, with U increasing linearly in x from the origin to the boundaries at $x = \pm 500$ μm (where periodic boundary conditions are applied). Initially, 10 000 particles are distributed uniformly in $-500 < x, y < 500$ μm, and Eqs. (2)–(4) simulated over long times. The particles are assumed to not interact with each other. After a slow migration, swimmers aggregate in the region of low fuel or diffusivity for $0 \leq U \leq 40$ $\mu\mathrm{m\,s^{-1}}$ [Fig. 5(a)]. Numerical solutions to the steady-state form of Eq. (5), modified to account for spatially varying swimming speed, show that the swimmer concentration increases with lower diffusivity, in agreement with an earlier model of bacterial chemotaxis [31]. The long-time distribution of swimmers is very different for $40 \leq U \leq 80$ $\mu\mathrm{m\,s^{-1}}$, which has the same gradient but a higher baseline [Fig. 5(b)]. Straight rods still aggregate but only weakly in the region of low fuel. The distribution of curved rods remains more uniform, because their diffusivity saturates at higher speeds.

Whether these predictions of migration and aggregation are correct remains an open question. Experiments using an H_2O_2-soaked agarose gel to set up a gradient have shown aggregation of swimmers at the gel after many hours [32]. This observation apparently disagrees with our predictions but may well be complicated by additional effects, such as large-scale gradient-driven flows [33] and localized changes in fluid viscosity. Further experiments using microfluidic techniques would shed more light on the possible mechanisms of aggregation in chemical gradients.

Near confining boundaries, swimmers with a tendency to turn are expected to aggregate near walls as they slide along the walls for prolonged periods [27]. While this effect may be useful for sorting curved rods according to their level of curvature, their stochastic flips must have a large effect on how they interact with walls and navigate through geometrically complex environments. Understanding how synthetic swimmers perform according to their shape, size, and environment may offer new directions to efficiently design, control, and operate microscopic devices in medical and technological applications, as well as serve as templates for new smart materials.

While synthetic biomimetic systems are worthy of study in their own right, it is often argued that they can shed light on their biological counterparts by being simpler and lacking the unknowns associated with behavior. Perhaps this is such a case. As implied already, the zooplankton *Daphnia* swims with angular velocity switching between two dominant values, and gliding organisms like the crescent-shaped *Toxoplasma gondii* can flip the body repeatedly [34], both of which move like the flipping rods described herein (despite fundamental differences in the mechanism of motility). An important aspect of our synthetic system is that the driving stochasticity can be precisely characterized as arising from thermal fluctuations with energy scale k_BT. Their relative contribution to the dynamics can be tuned so as to systematically explore the ensemble dynamics from stochastically dominated to more deterministic regimes.

We thank C. Chang, T. Majmudar, N. Moore, J. Palacci, L. Ristroph, and M. Ward for fruitful discussions. This work was supported by NSF (NYU MRSEC DMR-0820341, MRI-0821520, DMR-0923251, DMS-0920930), DOE (DE-FG02-88ER25053), and AFOSR (FA-9550-11-1-0032).

[1] G. A. Ozin, I. Manners, S. Fournier-Bidoz, and A. Arsenault, Adv. Mater. **17**, 3011 (2005).
[2] A. Goel and V. Vogel, Nat. Nanotechnol. **3**, 465 (2008).
[3] J. Wang, ACS Nano **3**, 4 (2009).
[4] S. J. Ebbens and J. R. Howse, Soft Matter **6**, 726 (2010).
[5] S. Balasubramanian, D. Kagan, C. M. Jack Hu, S. Campuzano, M. J. Lobo-Castañon, N. Lim, D. Y. Kang, M. Zimmerman, L. Zhang, and J. Wang, Angew. Chem., Int. Ed. **50**, 4161 (2011).
[6] L. Zhang, K. E. Peyer, and B. J. Nelson, Lab Chip **10**, 2203 (2010).

[7] S. Sundararajan, P. E. Lammert, A. W. Zudans, V. H. Crespi, and A. Sen, Nano Lett. **8**, 1271 (2008).
[8] W. F. Paxton, K. C. Kistler, C. C. Olmeda, A. Sen, S. K. St. Angelo, Y. Cao, T. E. Mallouk, P. E. Lammert, and V. H. Crespi, J. Am. Chem. Soc. **126**, 13 424 (2004).
[9] Y. Wang, R. M. Hernandez, D. J. Bartlett, Jr., J. M. Bingham, T. R. Kline, A. Sen, and T. E. Mallouk, Langmuir **22**, 10 451 (2006).
[10] R. Laocharoensuk, J. Burdick, and J. Wang, ACS Nano **2**, 1069 (2008).
[11] A. B. Braunschweig, A. L. Schmucker, W. D. Wei, and C. A. Mirkin, Chem. Phys. Lett. **486**, 89 (2010).
[12] R. Liu and A. Sen, J. Am. Chem. Soc. **133**, 20 064 (2011).
[13] W. Gao, A. Uygun, and J. Wang, J. Am. Chem. Soc. **134**, 897 (2012).
[14] L. Qin, M. J. Banholzer, X. Xu, L. Huang, and C. A. Mirkin, J. Am. Chem. Soc. **129**, 14 870 (2007).
[15] T. Mirkovic, N. S. Zacharia, G. D. Scholes, and G. A. Ozin, Small **6**, 159 (2010).
[16] J. G. Gibbs and Y. P. Zhao, Small **5**, 2304 (2009).
[17] J. G. Gibbs, S. Kothari, D. Saintillan, and Y. P. Zhao, Nano Lett. **11**, 2543 (2011).
[18] A. A. Solovev, W. Xi, D. H. Gracias, S. Harazim, C. Deneke, S. Sanchez, and O. G. Schmidt, ACS Nano **6**, 1751 (2012).
[19] B. R. Martin, D. J. Dermody, B. D. Reiss, M. Fang, L. A. Lyon, M. J. Natan, and T. E. Mallouk, Adv. Mater. **11**, 1021 (1999).
[20] M. J. Banholzer, L. Qin, J. E. Millstone, K. D. Osberg, and C. A. Mirkin, Nat. Protoc. **4**, 838 (2009).
[21] J. L. Moran and J. D. Posner, J. Fluid Mech. **680**, 31 (2011).
[22] D. Saintillan and M. J. Shelley, Phys. Rev. Lett. **99**, 058102 (2007).
[23] S. Kim, Int. J. Multiphase Flow **12**, 469 (1986).
[24] If the curved rods are more than a height $\sim\Delta h$ above the substrate, we anticipate a change in the nature of the system, because they could then rotate freely around their long axis without raising their center of mass. This would not yield two stable states or stochastic flipping between them as observed in our experiments and consequently modeled by our theory.
[25] M. Doi and S. F. Edwards, *The Theory of Polymer Dynamics* (Oxford University, New York, 1988).
[26] J. R. Howse, R. A. L. Jones, A. J. Ryan, T. Gough, R. Vafabakhsh, and R. Golestanian, Phys. Rev. Lett. **99**, 048102 (2007).
[27] S. van Teeffelen and H. Löwen, Phys. Rev. E **78**, 020101 (2008).
[28] L. Haeggqwist, L. Schimansky-Geier, I. M. Sokolov, and F. Moss, Eur. Phys. J. Special Topics **157**, 33 (2008).
[29] A. Ordemann, G. Balazsi, and F. Moss, Physica (Amsterdam) **325A**, 260 (2003).
[30] C. Weber, I. M. Sokolov, and L. Schimansky-Geier, Phys. Rev. E **85**, 052101 (2012).
[31] M. J. Schnitzer, S. M. Block, H. C. Berg, and E. M. Purcell, Symp. Soc. Gen. Microbiol. **46**, 15 (1990).
[32] Y. Hong, N. M. K. Blackman, N. D. Kopp, A. Sen, and D. Velegol, Phys. Rev. Lett. **99**, 178103 (2007).
[33] Y. Hong, D. Velegol, N. Chaturvedi, and A. Sen, Phys. Chem. Chem. Phys. **12**, 1423 (2010).
[34] S. Håkansson, H. Morisaki, J. Heuser, and L. D. Sibley, Mol. Biol. Cell **10**, 3539 (1999).